

Frequency comb assisted two-photon vibrational spectroscopy

JUHO KARHU,¹ MARKKU VAINIO,^{1,2} MARKUS METSÄLÄ,¹ AND LAURI HALONEN^{1,*}

¹Department of Chemistry, University of Helsinki, P.O. Box 55, FI-00014 University of Helsinki, Finland

²VTT Technical Research Centre of Finland Ltd., Centre of Metrology MIKES, P.O. Box 1000, FI-02044 VTT, Finland

*lauri.halonen@helsinki.fi

We report a setup for high-resolution two-photon spectroscopy using a mid-infrared continuous wave optical parametric oscillator (CW-OPO) and a near-infrared diode laser as the excitation sources, both of which are locked to fully stabilized optical frequency combs. The diode laser is directly locked to a commercial near-infrared optical frequency comb using an optical phase-locked loop. The near-infrared frequency comb is also used to synchronously pump a degenerate femtosecond optical parametric oscillator to produce a fully stabilized mid-infrared frequency comb. The beat frequency between the mid-infrared comb and the CW-OPO is then stabilized through frequency locking. We used the setup to measure a double resonant two-photon transition to a symmetric vibrational state of acetylene with a sub-Doppler resolution and high signal-to-noise ratio.

© 2017 Optical Society of America. One print or electronic copy may be made for personal use only. Systematic reproduction and distribution, duplication of any material in this paper for a fee or for commercial purposes, or modifications of the content of this paper are prohibited.

OCIS codes: (120.0120) Instrumentation, measurement, and metrology; (300.6320) Spectroscopy, high-resolution; (300.6340) Spectroscopy, infrared; (190.4970) Parametric oscillators and amplifiers.

References and links

1. R. Z. Martínez, D. Bermejo, G. Di Lonardo, and L. Fusina, "High resolution stimulated Raman spectroscopy from collisionally populated states after optical pumping: the $3\nu_2 \leftarrow 2\nu_2$ and $\nu_2 + 2\nu_4 + \nu_5 \leftarrow 2\nu_4 + \nu_5$ Q branches of $12C_2H_2$ and the $3\nu_2 \leftarrow 2\nu_2$ Q branch of $12C_2D_2$," *J. Raman Spectrosc.* **48**(2), 251-257 (2017).
2. M. Siltanen, M. Metsälä, M. Vainio, and L. Halonen, "Experimental observation and analysis of the $3\nu_1$ (Σ_g) stretching vibrational state of acetylene using continuous-wave infrared stimulated emission," *J. Chem. Phys.* **139**(5), 054201 (2013).
3. J. Karhu, J. Nauta, M. Vainio, M. Metsälä, S. Hoekstra, and L. Halonen, "Double resonant absorption measurement of acetylene symmetric vibrational states probed with cavity ring down spectroscopy," *J. Chem. Phys.* **144**(24), 244201 (2016).
4. W. K. Bischel, P. J. Kelly, and C. K. Rhodes, "Observation of Doppler-free two-photon absorption in the ν_3 bands of CH_3F ," *Phys. Rev. Lett.* **34**(6), 300-303 (1975).
5. A. Nishiyama, S. Yoshida, Y. Nakajima, H. Sasada, K. Nakagawa, A. Onae, and K. Minoshima, "Doppler-free dual-comb spectroscopy of Rb using optical-optical double resonance technique," *Opt. Express* **24**(22), 25894-25904 (2016).
6. M. Okubo, M. Misono, J. Wang, M. Baba, and H. Kato, "The Doppler-free two-photon absorption spectroscopy of naphthalene with Zeeman effects," *J. Chem. Phys.* **116**(21), 9293-9299 (2002).
7. M. Breton, N. Cyr, P. Tremblay, M. Tetu, and R. Boucher, "Frequency locking of a 1324 nm DFB laser to an optically pumped rubidium vapor," *IEEE Trans. Instrum. Meas.* **42**(2), 162-166 (1993).
8. F. Cappelli, I. Galli, S. Borri, G. Giusfredi, P. Cancio, D. Mazzotti, A. Montori, N. Akikusa, M. Yamanishi, S. Bartalini, and P. De Natale, "Subkilohertz linewidth room-temperature mid-infrared quantum cascade laser using a molecular sub-Doppler reference," *Opt. Lett.* **37**(23), 4811-4813 (2012).
9. E. V. Kovalchuk, D. Dekorsy, A. I. Lvovsky, C. Braxmaier, J. Mlynek, A. Peters, and S. Schiller, "High-resolution Doppler-free molecular spectroscopy with a continuous-wave optical parametric oscillator," *Opt. Lett.* **26**(18), 1430-1432 (2001).
10. I. Ricciardi, S. Mosca, M. Parisi, P. Maddaloni, L. Santamaria, P. De Natale, and M. De Rosa, "Sub-kilohertz linewidth narrowing of a mid-infrared optical parametric oscillator idler frequency by direct cavity stabilization," *Opt. Lett.* **40**(20), 4743-4746 (2015).

11. S. T. Cundiff and J. Ye, "Colloquium: Femtosecond optical frequency combs," *Rev. Mod. Phys.* **75**(1), 325-342 (2003).
 12. D. J. Jones, S. A. Diddams, J. K. Ranka, A. Stentz, R. S. Windeler, J. L. Hall, and S. T. Cundiff, "Carrier-envelope phase control of femtosecond mode-locked lasers and direct optical frequency synthesis," *Science* **288**(5466), 635-639 (2000).
 13. T. Udem, R. Holzwarth, and T. W. Hänsch, "Optical frequency metrology," *Nature* **416**(6877), 233-237 (2002).
 14. E. Benkler, F. Rohde, and H. R. Telle, "Endless frequency shifting of optical frequency comb lines," *Opt. Express* **21**(5), 5793-5802 (2013).
 15. T. Fordell, A. E. Wallin, T. Lindvall, M. Vainio, and M. Merimaa, "Frequency-comb-referenced tunable diode laser spectroscopy and laser stabilization applied to laser cooling," *Appl. Opt.* **53**(31), 7476-7482 (2014).
 16. M. Vainio and L. Halonen, "Mid-infrared optical parametric oscillators and frequency combs for molecular spectroscopy," *Phys. Chem. Chem. Phys.* **18**(6), 4266-4294 (2016).
 17. A. Schliesser, N. Picque, and T. W. Hänsch, "Mid-infrared frequency combs," *Nat. Photonics* **6**(7), 440-449 (2012).
 18. F. Adler, K. C. Cossel, M. J. Thorpe, I. Hartl, M. E. Fermann, and J. Ye, "Phase-stabilized, 1.5 W frequency comb at 2.8–4.8 μm ," *Opt. Lett.* **34**(9), 1330-1332 (2009).
 19. V. Ulvila, C. R. Phillips, L. Halonen, and M. Vainio, "High-power mid-infrared frequency comb from a continuous-wave-pumped bulk optical parametric oscillator," *Opt. Express* **22**(9), 10535-10543 (2014).
 20. P. Maddaloni, P. Malara, G. Gagliardi, and P. De Natale, "Mid-infrared fibre-based optical comb," *New J. Phys.* **8**(11), 262 (2006).
 21. A. G. Griffith, R. K. W. Lau, J. Cardenas, Y. Okawachi, A. Mohanty, R. Fain, Y. H. D. Lee, M. Yu, C. T. Phare, C. B. Poitras, A. L. Gaeta, and M. Lipson, "Silicon-chip mid-infrared frequency comb generation," *Nat. Commun.* **6**, 6299 (2015).
 22. A. Hugi, G. Villares, S. Blaser, H. C. Liu, and J. Faist, "Mid-infrared frequency comb based on a quantum cascade laser," *Nature* **492**(7428), 229-233 (2012).
 23. N. Leindecker, A. Marandi, R. L. Byer, K. L. Vodopyanov, J. Jiang, I. Hartl, M. Fermann, and P. G. Schunemann, "Octave-spanning ultrafast OPO with 2.6-6.1 μm instantaneous bandwidth pumped by femtosecond Tm-fiber laser," *Opt. Express* **20**(7), 7046-7053 (2012).
 24. N. Leindecker, A. Marandi, R. L. Byer, and K. L. Vodopyanov, "Broadband degenerate OPO for mid-infrared frequency comb generation," *Opt. Express* **19**(7), 6296-6302 (2011).
 25. I. Ricciardi, E. De Tommasi, P. Maddaloni, S. Mosca, A. Rocco, J. J. Zondy, M. De Rosa, and P. De Natale, "Frequency-comb-referenced singly-resonant OPO for sub-Doppler spectroscopy," *Opt. Express* **20**(8), 9178-9186 (2012).
 26. M. Vainio, M. Merimaa, and L. Halonen, "Frequency-comb-referenced molecular spectroscopy in the mid-infrared region," *Opt. Lett.* **36**(21), 4122-4124 (2011).
 27. J. Peltola, M. Vainio, T. Fordell, T. Hieta, M. Merimaa, and L. Halonen, "Frequency-comb-referenced mid-infrared source for high-precision spectroscopy," *Opt. Express* **22**(26), 32429-32439 (2014).
 28. I. Galli, S. Bartalini, P. Cancio, F. Cappelli, G. Giusfredi, D. Mazzotti, N. Akikusa, M. Yamanishi, and P. De Natale, "Mid-infrared frequency comb for broadband high precision and sensitivity molecular spectroscopy," *Opt. Lett.* **39**(17), 5050-5053 (2014).
 29. A. Nishiyama, K. Nakashima, A. Matsuba, and M. Misono, "Doppler-free two-photon absorption spectroscopy of rovibronic transition of naphthalene calibrated with an optical frequency comb," *J. Mol. Spectrosc.* **318**, 40-45 (2015).
 30. J. E. Bjorkholm and P. F. Liao, "Resonant enhancement of two-photon absorption in sodium vapor," *Phys. Rev. Lett.* **33**(3), 128-131 (1974).
 31. D. Romanini, A. A. Kachanov, N. Sadeghi, and F. Stoeckel, "CW cavity ring down spectroscopy," *Chem. Phys. Lett.* **264**(3), 316-322 (1997).
 32. M. Siltanen, M. Vainio, and L. Halonen, "Pump-tunable continuous-wave singly resonant optical parametric oscillator from 2.5 to 4.4 μm ," *Opt. Express* **18**(13), 14087-14092 (2010).
 33. S. T. Wong, K. L. Vodopyanov, and R. L. Byer, "Self-phase-locked divide-by-2 optical parametric oscillator as a broadband frequency comb source," *J. Opt. Soc. Am. B* **27**(5), 876-882 (2010).
 34. M. Vainio and J. Karhu, "Fully stabilized mid-infrared frequency comb for high-precision molecular spectroscopy," *Opt. Express* **25**(4), 4190-4200 (2017).
 35. J. E. Bjorkholm and P. F. Liao, "Line shape and strength of two-photon absorption in an atomic vapor with a resonant or nearly resonant intermediate state," *Phys. Rev. A* **14**(2), 751-760 (1976).
 36. H. K. Holt, "Frequency-correlation effects in cascade transitions involving stimulated emission," *Phys. Rev. Lett.* **19**(22), 1275-1277 (1967).
 37. D. Jacquemart, J. Y. Mandin, V. Dana, C. Claveau, J. Vander Auwera, M. Herman, L. S. Rothman, L. Régalia-Jarlot, and A. Barbe, "The IR acetylene spectrum in HITRAN: update and new results," *J. Quant. Spectrosc. Radiat. Transfer* **82**(1-4), 363-382.
 38. J. J. Hillman, D. E. Jennings, G. W. Halsey, S. Nadler, and W. E. Blass, "An infrared study of the bending region of acetylene," *J. Mol. Spectrosc.* **146**(2), 389-401 (1991).
-

1. Introduction

Spectroscopy methods based on stimulated two-photon transitions, such as two-photon absorption, stimulated emission probing, and stimulated Raman spectroscopy, allow accessing energy states in which typical single photon excitations are forbidden under spectroscopic selection rules [1-3]. Stimulated two-photon transition can be used to measure spectral features at sub-Doppler resolution, without the need for cooling or molecular jets [4]. The inherent sub-Doppler resolution has been utilized, for example, in probing minute spectral features, such as hyperfine transitions and Zeeman splitting [5, 6], and in laser stabilization [7]. For typical laser sources, the measurement resolution may become limited by the linewidths of the exciting lasers. Therefore, light sources with narrow linewidths and precise wavelength tuning are required to take the full advantage of the sub-Doppler resolution. Achieving these requirements generally calls for active stabilization of the laser wavelengths.

Classical frequency references for the stabilization include atomic or molecular resonances [8], more stable reference lasers [9], and high-finesse cavities [10]. Molecular resonances and reference lasers work over limited wavelength ranges, and while an optical cavity simultaneously covers a wide spectral range, it is susceptible to thermal and mechanical effects and the absolute positions of the cavity resonances are generally unknown. Optical frequency combs work as ideal frequency references, as they cover a wide wavelength region with narrow linewidth laser lines [11]. A fully stabilized comb can be used to determine a laser wavelength with high precision and accuracy [12, 13]. The frequency comb technology is already highly developed in the near-infrared region, and therefore near-infrared combs are commonly used for accurate wavelength measurement and as references in laser locking schemes [14, 15]. For applications in molecular spectroscopy, an important prospect is the expansion of frequency comb technology into the mid-infrared region [16, 17]. Mid-infrared frequency combs are under constant development, and several methods for producing them have already been demonstrated [18-24].

In this article, we present a frequency comb assisted measurement setup for probing two-photon vibrational transitions. The setup uses two light sources: an external cavity diode laser (ECDL) and a mid-infrared optical parametric oscillator (CW-OPO). Both sources are stabilized using an optical frequency comb reference. The ECDL is directly locked to a commercial fully stabilized near-infrared frequency comb with an optical phase-locked loop (OPPL). Because of the availability of commercial near-infrared frequency combs, the stabilization of a mid-infrared CW-OPO is often done indirectly, for example by locking both the pump and signal wavelengths with the comb. This also produces a stable idler wavelength due to the conservation of energy [25, 26]. A more direct method uses second harmonic generation to convert some of the mid-infrared idler power into a near-infrared beam, which is then referenced to the frequency comb [27]. Here, we stabilize the mid-infrared CW-OPO directly to a phase-stabilized mid-infrared frequency comb, produced by half-harmonic generation with a synchronously pumped degenerate femtosecond OPO (fs-OPO). Similar methods based on a mid-infrared comb produced by difference frequency generation have previously been used to stabilize quantum cascade lasers working in the mid-infrared region [28].

Frequency combs have been utilized in direct comb and comb assisted Doppler-free two-photon spectroscopy of excited electronic states in atoms and molecules [5, 29]. Here, we have used our comb assisted measurement setup for vibrational spectroscopy, to access a symmetric vibrational state of acetylene using two-photon absorption. The target state, $\nu_1+2\nu_3$ in normal mode notation, is inaccessible by single photon excitations from the vibrational ground state. The rovibrational transitions are measured with a signal-to-noise ratio (SNR) surpassing previously reported measurements of this state. Due to the stabilization of the exciting lasers, the sub-Doppler line shapes of the transitions are resolved, and the line center and shape parameters can be extracted with high precision and accuracy.

2. Experimental setup

An overview of the two-photon measurement setup is presented Fig. 1. Our spectrometer uses a nondegenerate double resonant configuration, where two different light sources provide the two photons for the transition. One of the light sources is the mid-infrared CW-OPO, which emits in the spectral region of the strong fundamental CH stretching vibrations. Tuning the exciting wavelengths near strong resonant transitions enhances the two-photon transition strength [30]. The second light source is an external cavity diode laser emitting in the near-infrared region, where we can take advantage of highly developed cavity-enhanced detection methods to increase the sensitivity. Here we are using continuous-wave cavity ring-down spectroscopy (CRDS) [31].

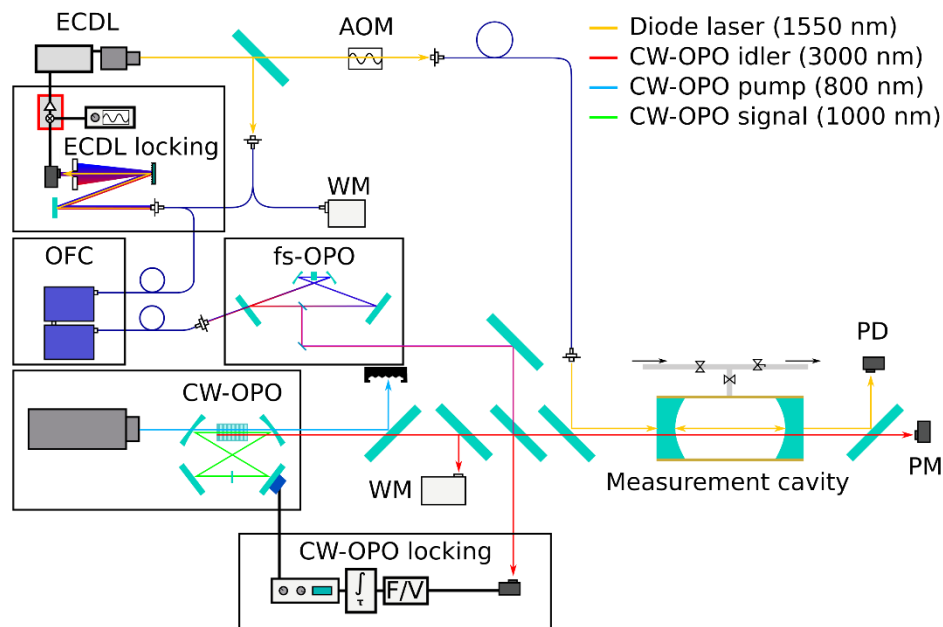


Fig. 1. Schematic overview of the setup. A diode laser (ECDL) is locked to a commercial fully stabilized near-infrared frequency comb (OFC) with an optical phase-locked loop. An acousto-optical modulator (AOM) is used to initiate ring-down events. The CW-OPO idler is locked to a mid-infrared comb produced by a synchronously pumped femtosecond OPO (fs-OPO). Their beat note is measured and fed through a frequency-to-voltage converter (F/V) to an integrator, which tunes the CW-OPO cavity length via a piezo actuator, to stabilize the beat note. After the measurement cavity, a power meter (PM) determines the transmitted idler power and a photodiode (PD) measures the ring-down signals at the ECDL wavelength. Wavemeters (WM) are used for approximate wavelength measurements. They also help to determine the frequency comb mode numbers and the fs-OPO carrier-envelope offset frequency.

2.1. ECDL locking

The ECDL (Velocity 6328, New Focus) wavelength is tunable between 1520 and 1570 nm. The diode laser is locked to a commercial fully stabilized optical frequency comb (FC1500-250-WG, Menlo Systems) with a phase-locked loop (Fig. 2). A beam sampler sends a small portion of the diode laser output to a polarization maintaining optical fiber. The sampled beam and the frequency comb are overlaid with a 50/50 fiber coupler. The beams are coupled out of the fiber and diffracted by a reflective grating to filter about 1.5 nm wide portion of the comb

spectrum around the ECDL wavelength. The filtered comb and the ECDL beam sample are again coupled into a fiber and sent to a fast photodiode. The beat note measured by the detector is amplified, filtered and sent to a commercial optical phase-lock filter (mFALC 110, TOPTICA Photonics). The beat note frequency is phase-locked to a local oscillator frequency provided by a signal generator, which is referenced to the same time base as the frequency comb. The output from the locking electronics is separated into three parts: fluctuations below 100 kHz are corrected by the laser current through the laser control electronics, faster corrections are made through a direct connection to the laser head, and the laser cavity piezo is used to counteract long-term drifts. The CRDS setup requires that the main output from ECDL is directed through an acousto-optical modulator (AOM), which is used to shut off the ECDL output at nanosecond scale to initiate the ring-down events. The ECDL frequency in the measurement cavity (f_{DL}) is given by $f_{DL} = f_{ceo} + nf_r + \Delta f - f_{AOM}$, where f_{ceo} is the frequency comb carrier-envelope-offset frequency, nf_r is the frequency comb repetition rate times an integer n , Δf is the frequency of the beat note, and f_{AOM} is the frequency shift from the AOM. The first negative order of the AOM was used so the ECDL frequency decreased by f_{AOM} , which was 80.00112 MHz, as measured with a frequency counter. The repetition rate of the frequency comb is 250 MHz and the carrier-envelope-offset is 10 MHz. The frequency comb time scale is referenced to the SI-second through a GPS (Global Positioning System) reference frequency generator (GPS-8-12, Menlo Systems).

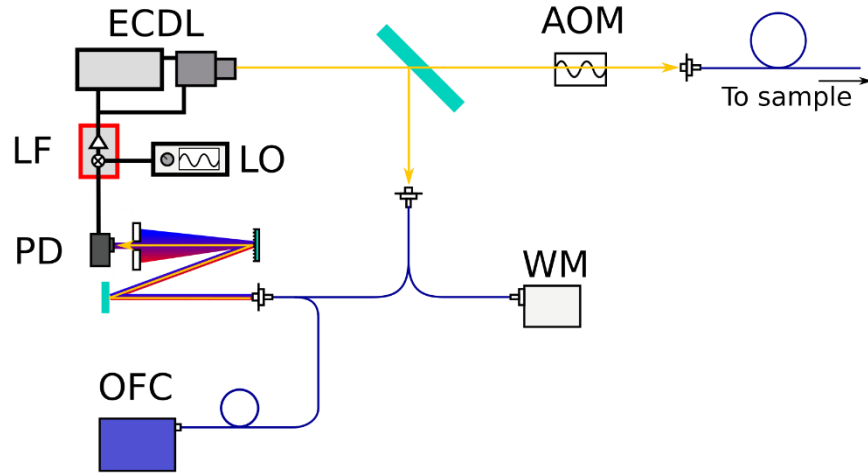


Fig. 2. Schematic layout of the ECDL phase lock. The ECDL and optical frequency comb (OFC) beams are overlaid with a 50/50-fiber coupler. The comb spectrum around the ECDL is separated from the rest of the comb with a reflective grating and the beat note between the ECDL and OFC lines is detected with a photodiode (PD). The beat note is mixed with a local oscillator (LO) frequency from a signal generator. The locking filters (LF) tune the ECDL to bring the difference frequency between the beat note and the LO frequencies to zero.

When unlocked, the signal-to-noise ratio of the beat note between the ECDL and the filtered frequency comb was about 30 dB (resolution bandwidth 100 kHz). When locked, the carrier linewidth in the beat note spectrum was less than 10 Hz, limited by the resolution of the radio spectrum analyzer used to measure the spectrum (Fig. 3).

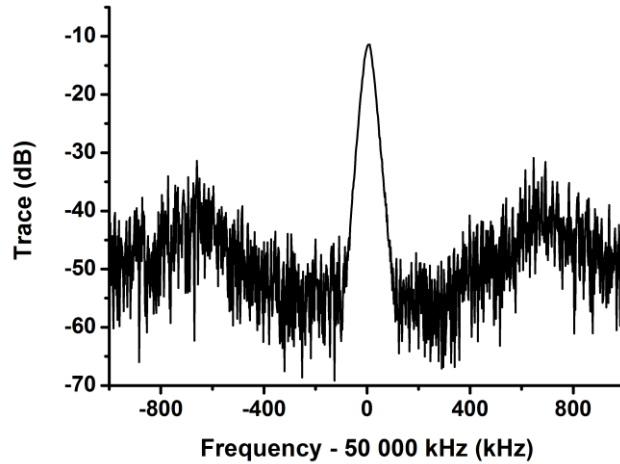


Fig. 3. Spectrum of the beat note between the ECDL and the frequency comb when the phase-lock is established. The resolution bandwidth (RBW) was 30 kHz. The frequency axis provides the difference from the locking point (50 MHz).

2.2. CW-OPO locking

The CW-OPO is a singly-resonant OPO in a four mirror bow-tie configuration. The nonlinear medium is a 5 cm long periodically poled, MgO doped lithium niobate crystal. The CW-OPO is pumped using a continuous-wave titanium sapphire ring-laser (MBR-PS, Coherent), emitting light at around 800 nm. By tuning the pump wavelength, the idler wavelength can be tuned between 2.5 and 4.4 μm [32].

The same commercial near-infrared frequency comb, which is used as the direct reference for the ECDL, is amplified and used to pump an fs-OPO. The nonlinear medium is a 1 mm long periodically poled lithium niobate crystal. The free spectral range of the fs-OPO cavity is synchronized to the repetition rate of the comb. Pumping the fs-OPO with a frequency comb generates a comb structure at both the signal and the idler wavelengths and the fs-OPO is working in the degenerate regime, where the signal and the idler spectra overlap and become indistinguishable. This generates a phase-stabilized mid-infrared frequency comb [33], which in our case spanned a 400 nm wide spectrum around 3 μm . The output power from the fs-OPO is about 20 mW after filtering out the residual pump beam. Details of the fs-OPO comb can be found in [34].

Overview of the CW-OPO locking setup is presented in Fig. 4. The output beam from the fs-OPO and a beam sample of the CW-OPO output, reflected from a CaF_2 -surface, were overlaid on a fast MIR photodiode (PVI-2TE-5, VIGO), with a bandwidth up to about 30 MHz. The beat note was sent to a frequency-to-voltage converter and the generated voltage was used as an error signal for an integrator. The integrator controlled the CW-OPO cavity length via a piezo actuator attached to one of the cavity mirrors, in order to keep the voltage constant and hence the beat note frequency stable at around 15 MHz. The actual beat note frequency was followed with a frequency counter. The CW-OPO frequency (f_{OPO}) is then given by $f_{\text{OPO}} = f_{\text{ceo,MIR}} + nf_r + \Delta f$, where nf_r , and Δf are as defined before for the ECDL locking. The fs-OPO carrier-envelope-offset $f_{\text{ceo,MIR}}$ can be either $f_{\text{ceo,MIR}} = f_{\text{ceo}} / 2$ or $f_{\text{ceo,MIR}} = (f_{\text{ceo}} + f_r) / 2$ [33], and is determined separately by an approximate measurement of the CW-OPO frequency using a calibrated wavemeter (WA-1500-IR, EXFO) and a spectrum analyzer (WA-650, EXFO).

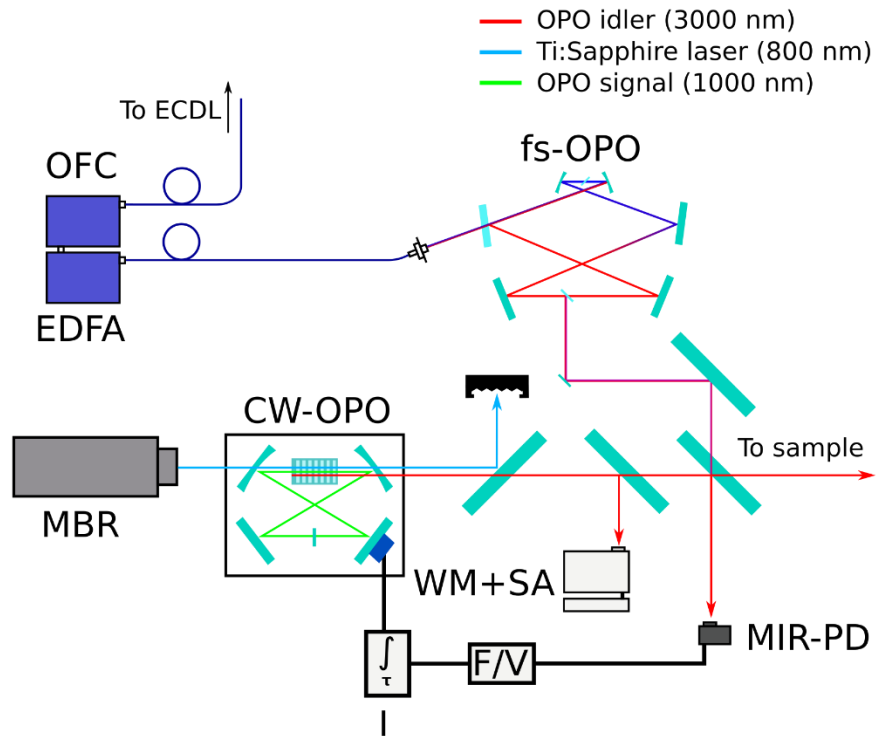


Fig. 4. Schematic overview of the CW-OPO locking. A near-infrared frequency comb (OFC) is amplified (EDFA) and used to synchronously pump a pulsed OPO (fs-OPO). The idler beam from a continuous-wave mid-infrared OPO (CW-OPO), pumped with a CW Ti:Sapphire laser (MBR), is overlaid with the fs-OPO beam and their beat note is measured with a photodetector (MIR-PD). The beat note frequency is converted into an input signal for an integrator (I) with a frequency-to-voltage converter circuit (F/V). The integrator tunes the CW-OPO cavity with a piezo-actuator to stabilize the beat note frequency. The CW-OPO wavelength is also measured with a wavemeter connected to a spectrum analyzer (WM+SA).

When the locking was established, the linewidth of the beat note was measured to be about 500 kHz with a sweep time of 150 ms and about 1.5 MHz with a sweep time of 1 second with a spectrum analyzer (Fig. 5). The standard deviation of the beat note frequency was about 90 kHz as measured with a frequency counter over a longer period of about 20 minutes. For comparison, the short term linewidth of the free running CW-OPO was the same as when locked, but over a few seconds, the wavelength instability was on the order of 10 MHz, mainly due to drifting of the pump laser.

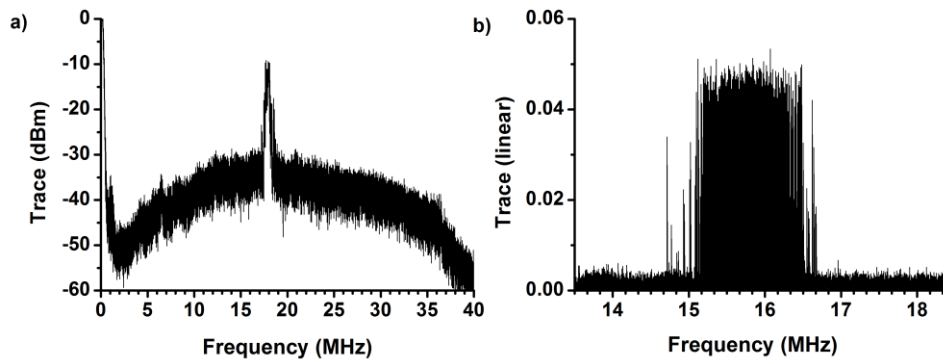


Fig. 5. Spectra of the beat note between the CW-OPO and the fs-OPO when the CW-OPO was locked, measured with a sweep time of a) 150 ms (100 kHz RBW) and b) 1 s (100 kHz RBW). Figure a) is a direct trace from the spectrum analyzer, showing also the background noise and the detector bandwidth. In figure b), the power scale is linear and the background has been subtracted.

3. Spectroscopic measurements

3.1. Two-photon setup

We used the setup to measure a transition to the rotational state $J = 18$ of the vibrational state $\nu_1+2\nu_3$ (Fig. 6) in acetylene (C_2H_2). We employ here the standard spectroscopic notation, where ν_1 is the symmetric and ν_3 the anti-symmetric CH-stretching vibration. A single photon transition to this state, from the vibrational ground state, is forbidden. The CW-OPO wavelength is tuned to the side of the transition P(18) of the fundamental band of the ν_3 stretching vibration and the frequency lock between the CW-OPO and the fs-OPO is turned on. The ECDL is locked to the near-infrared comb and the ECDL wavelength is scanned over the second transition: line R(17) of the band $\nu_1+2\nu_3 \leftarrow \nu_3$. Since both light sources are referenced to the same comb, we cannot scan the ECDL by tuning the comb repetition rate, without also changing the CW-OPO wavelength. Instead, the ECDL is scanned by tuning the local oscillator frequency of the phase-locked loop [15]. This simple tuning method gives us precise control over the ECDL wavelength, but a new scan has to be started when passing over the comb lines. The scanning was typically done in steps of 200 kHz, and at each step, 50 ring-down times were averaged.

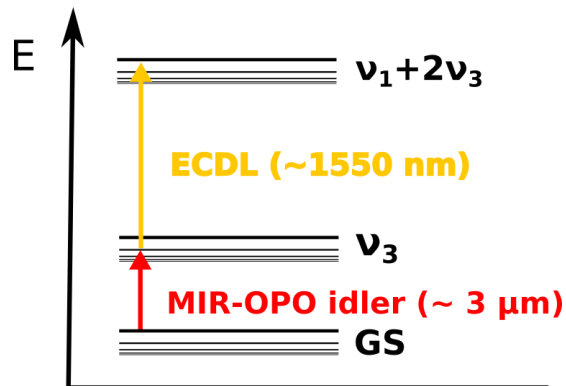


Fig. 6. Energy diagram showing the principle of the spectroscopic measurement. A CW-OPO idler wavelength is tuned to the side of a strong mid-infrared transitions and the ECDL is scanned over near-infrared transition, where the lower state is the one that the CW-OPO is pumping. The symbol GS stands for the vibrational ground state.

A static gas sample of acetylene is taken into a high-finesse ring-down cavity for the measurement, with a pressure below 1 torr (1 torr is about 133 Pa). The ring-down cavity finesse is about 150 000 at the ECDL wavelength, but it transmits the mid-infrared CW-OPO beam (Fig. 7). The ECDL and CW-OPO power entering the ring-down cavity is about 10 and 30 mW, respectively. The ECDL and the cavity are brought into resonance by periodically tuning the cavity length with a piezo actuator over the cavity free spectral range, at a frequency of 20 Hz. After the intracavity power starts to rise and surpasses a threshold value, the ECDL input into the cavity is cut off using the AOM. The cavity decay time is recorded with a high-speed photodetector (D100, RedWave Labs). The least-squares fitting and extracting the decay constants are done using a LabView (National Instruments) program. The two-photon absorption signal can be seen as a drop in the decay time of the ECDL power inside the cavity, as the absorption adds to the cavity losses. The background is measured with the CW-OPO turned off.

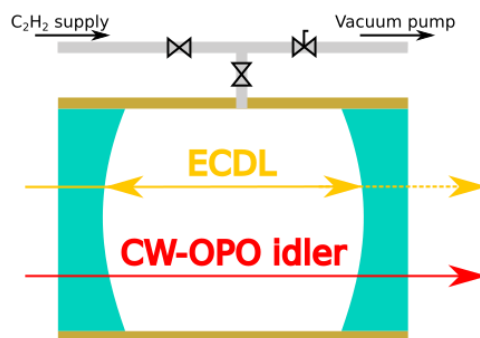


Fig. 7. Schematic representation of the spectroscopic measurement. The ECDL and the CW-OPO beams are overlaid and sent through the cavity. The cavity mirrors are highly reflective at the ECDL wavelength, but not at the CW-OPO wavelength. The measurement cavity is filled with a sample of acetylene gas at a pressure below 1 torr.

3.2. Results

Figure 8 shows a CRDS spectrum of the R(17) line of the transition $v_1+2v_3 \leftarrow v_3$. As the ECDL forms a standing wave inside the linear cavity, it probes the two-photon transition with both counter-propagating waves. The CW-OPO is exciting a narrow component of the Doppler-profile of the fundamental transition, which has different Doppler-shifts in respect to the two counter-propagating ECDL waves inside the cavity. The shifts have the same magnitude, but opposite signs, and therefore the CRDS spectrum shows two peaks symmetrically around the line center. Both have Lorentzian profiles, but with different linewidths. Depending on whether ECDL and CW-OPO beams are co- or counter-propagating, there is a partial enhancement or cancellation of the residual Doppler-broadening [35, 36]. The measured line shapes were least-squares fitted with Lorentzian profiles to extract their center positions and widths. At a pressure of 0.2 torr, the linewidth (the full width at half maximum) of the narrow peak, corresponding to counter-propagating CW-OPO and ECDL, was 8.995 (65) MHz, and the width of the broader peak was 15.437 (73) MHz. The values in the parentheses, here and below, are one standard errors in the least significant digits.

The signal-to-noise ratio of the higher peak, defined here as the peak height divided by the standard deviation of the background signal, was about 1000. For reference, Fig. 9 shows the same transition line measured with free-running lasers. The spectrum shows only the narrower

of the two peaks, which corresponds to counter-propagating CW-OPO and ECDL. Here the scanning was done by tuning the ECDL cavity piezo. The step size was about 4 MHz, so that the scan would cross the transition line on a time scale where the CW-OPO stability would be acceptable. This also ensured that the step size was slightly larger than the linewidth of the ECDL, which was a few MHz on the time scale of a single step, which took less than 2 seconds. The SNR of the unlocked scan was about 60. Because the CW-OPO offset was slightly different for this measurement, the wavenumbers of the peaks in the two figures do not match exactly. The best previous measurement of this state, based on a stimulated emission setup, had an SNR of about 500 [2].

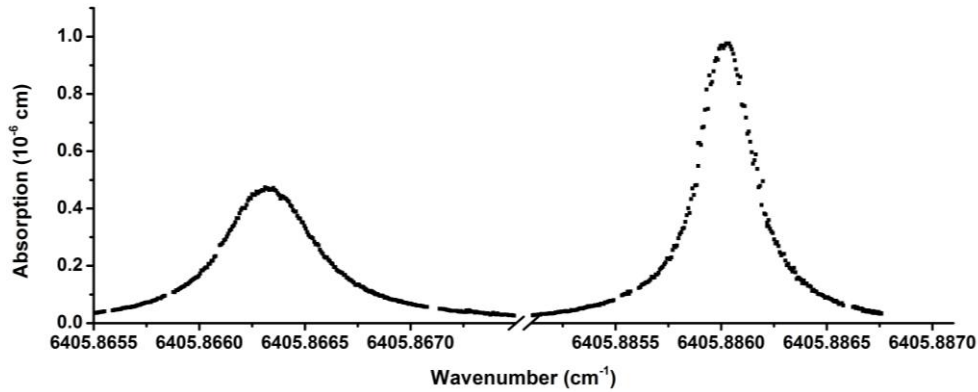


Fig. 8. Comb-assisted two-photon absorption spectrum of transition from the ground state to v_1+2v_3 , with a resonant intermediate state v_3 . The horizontal scale is the wavenumber of the ECDL as it is scanned over the second resonance. The appearance of two peaks is a result of the CW-OPO exciting a narrow Doppler-component to the intermediate state and the standing wave formed by the ECDL probes the Doppler-component with both counter-propagating waves. The broader spectrum on the left hand side corresponds to the case where the two photons come from co-propagating CW-OPO and ECDL waves, and the residual Doppler broadening is enhanced. In the narrow peak on the right hand side, the exciting waves are counter-propagating, partially canceling the residual Doppler-broadening. The small gaps in the spectra are points where the phase-locked loop had dropped and was re-established.

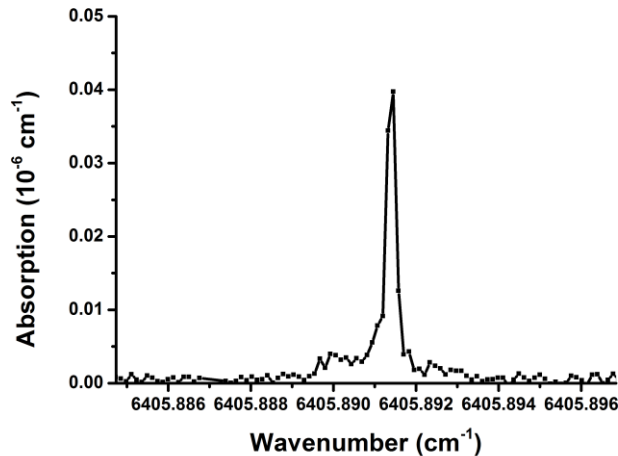


Fig. 9. Two-photon absorption spectrum with free-running CW-OPO and ECDL. The spectrum shows only the higher frequency peak, corresponding to counter-propagating CW-OPO and ECDL. The asymmetry of the peak is due to the long-term instability of the CW-OPO wavelength, as the scan over the peak takes about 10-20 s. The SNR is about 60.

Excluding possible asymmetries and pressure shifts in the two-photon transition profiles, which are small at these pressures, the line center is at the midpoint between the two peaks, giving it the value of 6405.87617729 (45) cm^{-1} . The one-standard error is from the uncertainty in the center positions of the Lorentzian fits. The Doppler shift of the excited velocity component can be resolved from the frequency difference of the two peaks in the CRDS spectrum, so the line center of the mid-infrared transition can also be calculated at the sub-Doppler level. Since the wider peak in the CRDS spectrum, corresponding to co-propagating CW-OPO and ECDL, was at lower energy, we know that the CW-OPO frequency corresponds to a negative Doppler-shift and is below the center frequency of the mid-infrared transition line. The CW-OPO wavenumber was determined to be 3251.081911 (3) cm^{-1} , where the uncertainty is limited by the standard deviation of the locked beat note frequency. This gives the line center as 3251.086908 (3) cm^{-1} , when the speed of the probed Doppler component is determined from the difference in the frequencies of the CRDS spectrum peaks. Previous measurements gives the line center as 3251.08683 cm^{-1} , with an accuracy reported as better than 0.001 cm^{-1} [37]. The total energy of the final rovibrational state, calculated as the sum of the two measured transition line centers and the rotational energy of the ground state [38], is 10059.186015 (31) cm^{-1} , where the precision is mostly limited by the uncertainty in the ground state rotational parameters. Previously measured effective band parameters of the final symmetric vibrational state predict the state energy to be 10059.1876 (10) cm^{-1} [3]. The measurement results are summarized in table 1.

Table 1. Measured transition line positions and the energy of the upper state

Transition	This work ^a	Reference
P(18), $\nu_3 \leftarrow$ Ground State (cm^{-1})	3251.086908 (3)	3251.08683 [37]
R(17), $\nu_1+2\nu_3 \leftarrow \nu_3$ (cm^{-1})	6405.87617729 (45)	-
Energy of the state $\nu_1+2\nu_3, J=18$ (cm^{-1})	10059.186015 (31) ^b	10059.1876 (10) ^c

^aThe values in the parentheses are one standard errors in least significant digits.

^bCalculated from the measured line positions and the ground state rotational energy [38].

^cCalculated with the band parameters from [3].

4. Conclusions

We have presented a frequency comb assisted setup for measuring infrared-infrared double resonant two-photon transitions. We reach high accuracy and precision by referencing the light sources, a near-infrared ECDL and a mid-infrared CW-OPO, against the same fully stabilized optical frequency comb. For our near-infrared source, we can directly establish a phase-locked loop to stabilize the beat between the diode laser and the comb by tuning the laser current, and reach relative linewidth below 10 Hz, as limited by the resolution of our spectral analyzer. The CW-OPO was referenced to a mid-infrared frequency comb produced by a degenerate fs-OPO, which was synchronously pumped using the near-infrared frequency comb. In this way, both light sources were linked to the same stabilized repetition rate and carrier envelope offset frequencies. With a simple frequency locking of the CW-OPO and fs-OPO beat, we could stabilize the long term linewidth of the CW-OPO to about 1.5 MHz.

The setup was used to measure a two-photon transition of acetylene to an infrared inactive vibrational state $\nu_1+2\nu_3$. With the frequency comb assisted measurement, we could resolve the shape of the sub-Doppler transition line, which was not achieved in our previous measurement with free running lasers, and precision of the line position measurement was increased by an order of magnitude [3]. The SNR was also improved by an order of magnitude compared to

when the light sources were free-running, and by an order of two compared to a measurement of the same state with previously the best sensitivity [2].

The precision of the line position measurement is limited by the CW-OPO frequency lock, which is based on a simple frequency-to-voltage converter. The beat note between the CW-OPO and the fs-OPO showed a standard deviation of 90 kHz when followed with a frequency counter during the measurement. The accuracy is ultimately limited by the GPS corrected reference oscillator, which links the time scales of the local oscillator of the phase-locked loop and stabilized frequencies of the frequency comb to the SI second. The accuracy of the GPS reference is reported to be better than 8×10^{-12} in one second, which translates to an accuracy of about 1.5 kHz at the ECDL wavelength.

By utilizing a more complex locking mechanism for the CW-OPO, the line position measurement could be improved. A short term linewidth down to sub-kilohertz level has been reached with Pound-Drever-Hall cavity locking [10], but the result does not directly translate to long term stability and lacks the absolute frequency reference offered by a stabilized frequency comb. A long term linewidth of less than 200 kHz has been achieved with phase-locking of CW-OPO pump and signal frequencies against a frequency comb [25]. Using a high bandwidth locking, together with the direct reference between CW-OPO idler and a mid-infrared comb presented here, we could expect similar or marginally better results, since the idler frequency stability would depend on the stability of only one beat note. However, a fast tuning element, such as an electro optic modulator, required for phase locking the CW-OPO was not available to us at this time.

Funding

CHEMS doctoral program of the University of Helsinki; the Finnish Cultural Foundation; the Academy of Finland (grant numbers #257479 and #294752); the Finnish Funding Agency of Technology and Innovation (TEKES, grant number #498/31/2015).